

## A Study on the Determination of the Appropriate Imaging Conditions in the Use of Scintillation Camera

Joon Huh

Dept. of Radiotechnology, Junior College of Public Health and Medical Technology, Korea University

Kwang Hyon, Kyong

Dept. of Radiotechnology, Shin Heung Junior College, Korea

抄 錄

### Scintillation Camera使用時 適正한 撮像條件의 設定에 關한 研究

高麗大學校 保健專門大學 放射線科

許 俊

信興實業專門大學 放射線科

慶 光 顯

Scintillation camera을 使用할때 良質의 畫像을 얻기 위하여 camera의 性能, 放射性藥劑의 特性, 그리고 適正한 撮像條件을 고려할 必要가 있다. 特히 RI像에 대한 撮像條件은 film의 性質, 像의 크기, 像의 濃度, window, 그리고 콜리메타 前面으로부터 距離 等에 따라서 左右된다. 이러한 要因들은 各々 畫像을 만드는 과정에 影響을 미치고 있다. 그러므로 像의 標準化와 撮像方法의 基準을 確立하기가 매우 어렵다. 고로 이러한 問題들을 解決하는 것은 Scintillation camera을 使用하는 核醫學의 檢査에 있어서 매우 重要하다. 著者는 이러한 點을 고려하여 一定한 像의 濃度를 얻을 수 있는 撮像條件에 對하여 實驗을 하였다.

實驗에 있어서 平行多孔型 콜리메타를 camera의 head에 附着시키고  $^{99m}\text{Tc}$  (3mCi)가 넣어져 있는 liver phantom을 콜리메타의 表面에 密着시켜 다음과 같은 方法에 의하여 撮像하였다. 즉, 一定한 像의 濃도를 얻을 수 있는 撮像條件을 찾아낼 目的으로 pre-

set time, image size, 콜리메타前面-phantom間 距離, 그리고 window을 各々 變化시키면서 phantom을 撮像하였으며, 特히 距離와 window에 있어서는 cold defects의 檢出能도 比較檢討하였다. 實驗結果는 다음과 같다.

1. C type film에 있어서 1.5의 濃度를 얻기 위해서는 7.5의 intensity에서 preset time은 60秒, image size는 .1.0, 콜리메타-phantom間 距離는 0 cm 그리고 window는 20%가 要求되고 있었다.
2. 片面乳劑 film의 preset time은 兩面乳劑 film보다 짧은 것으로 나타났다.
3. 像의 分解能은 image size가 작을수록, 콜리메타-phantom間 距離가 짧을수록, 그리고 window幅이 좁을수록 더욱 더 向上되고 있었다.
4. Cold defects의 檢出能은 image size가 작을수록, 콜리메타-phantom間 距離가 짧을수록, 그리고 window幅이 좁을수록 向上되고 있었다.

## 1. Introduction

When the scintillation camera is used, it is necessary to consider the performance of the camera, characteristics of a radiopharmaceuticals and the proper imaging conditions for the best possible images. Especially, the imaging conditions for RI images is dependent upon the film types, the image size, the image density, the window width and the distance from the surface of the collimator, etc.<sup>1)</sup> Each of these factors also has an effect on some of imaging forming procedures. Therefore it is difficult to set a standardization of the image and imaging methodology. However, to overcome these problems is very important in scintigraphic studies using scintillation camera. In consideration of these points, the author carried out an experiment on the imaging condition for a given image density.

## 2. Equipments and Materials

Scintillation camera: CGR Gammatome T 90000

Collimator: Low-energy, high resolution parallel multihole type

Phantom: Liver phantom/Picker Nuclear

Radionuclide: Technetium-99m

Film type: Single coating film (3 type) and Double coating film (1 type)

Densitometer: Sakura PDA-81

Automatic processor: Sakura New QX/200

## 3. Methods

A parallel multihole type collimator was attached to the camera head and liver phantom (Fig.1) filled with technetium-99m (3m Ci) was contacted with the surface of the collimator for these experiments. And all of images were taken by means of procedures as follows.

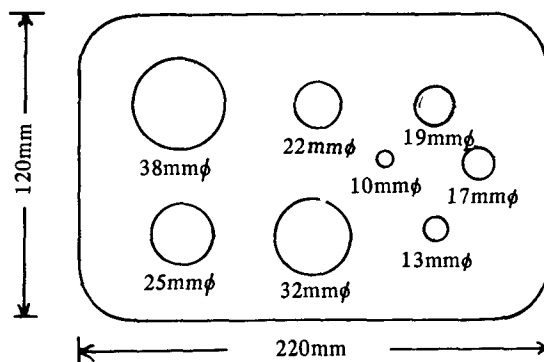


Fig. 1. Liver phantom/Picker Nuclear Each Circle is a Cold Area.

**1) The optimal preset time settings for a given image density**

The purpose of this experiment is to determine the preset time for a constant image density. All of RI images were formed with different preset time (30, 60, 100, 120, 150, 200 and 250 seconds) at each CRT intensity (6.5, 7.0, 7.5, 8.0 and 8.5). Four different types of film were used for the imaging procedures.

**2) The proper image size settings for a given image density**

In order to set the image size for a given image density, all pictures were performed with different image sizes (1.0, 1.2, 1.4, 1.6, 1.8 and 2.0) at the proper preset time determined from experiment 1. Four different types of film were also used in this imaging procedures.

**3) The appropriate settings distance of the surface of the collimator for a given image density**

To determine the appropriate distance from the face of the collimator for a constant image density, all images were taken with different distances from the face of the collimator (0.5, 10 and 15cm) at the preset time and image size selected from experiment 1 and 2. Also the image densities of cold areas were measured and the detectability of them was observed.

**4) The suitable window width settings for a given image density.**

To establish the suitable window width for a given image density, all photographs were taken with different window widths (15, 20, 30 and 40%) at the preset time, image size and the distance from the surface of the collimator obtained from experiment 1, 2 and 3. Also image densities of cold areas were measured and the detectability of them was observed.

**4. Results**

**1) The optimal preset time settings for a given image density**

Fig.2 indicates the examples of images taken by employing the different preset time at the intensity of 7.5. A point was reached, as evidence by figures, where the preset time was too extended, the image densities and resolution of images became saturated and informations of the images were lost. And as the preset time increased, the image density became more high as depicted in Fig.3. Table 1 shows the optimal preset time for a image density of 1.3 to 1.6 at the different intensity. For examples, when the CRT intensity was fixed upon 7.5, the preset time for a image density of 1.5 was 94 seconds in the case of A type film, 82 seconds in case of B type film, 60 seconds in the case of C type film and 205 seconds with respect to D type of film.

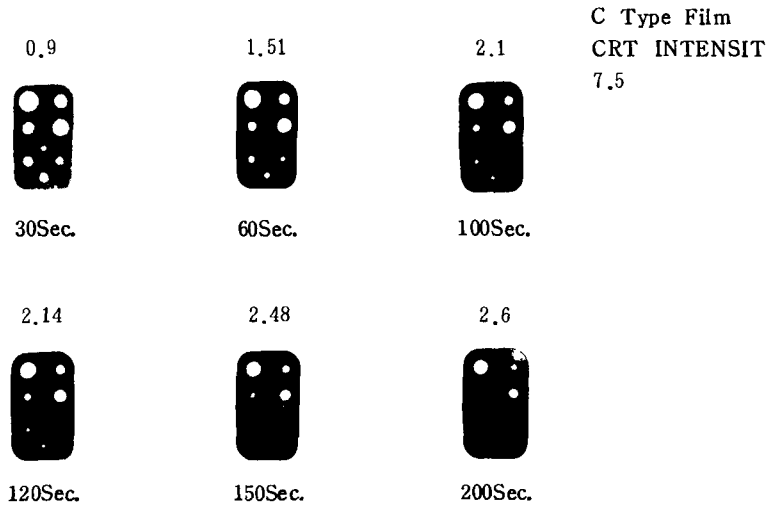


Fig. 2. Images of liver phantom taken by employing different preset time at the CRT intensity of 7.5

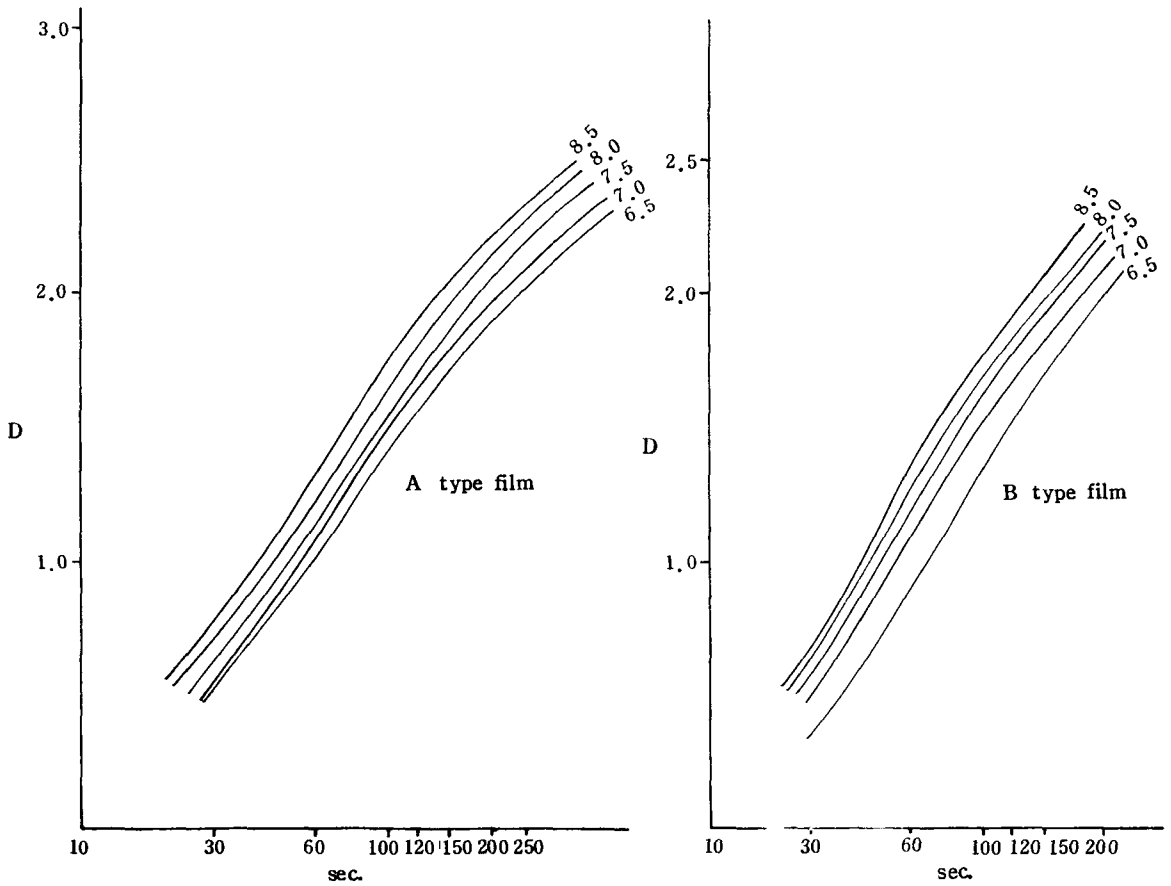


Fig. 3. Densities curve for image as function of preset time for four types of films (A, B, C and D type film)

In this cases, it showed that the preset time of single emulsion films (A,B,C type) was found to be short than that of double emulsion film. And then, among the single coating films, the preset time of C type film was too short and that of A type film was too long at each intensity, as represented in Table 1.

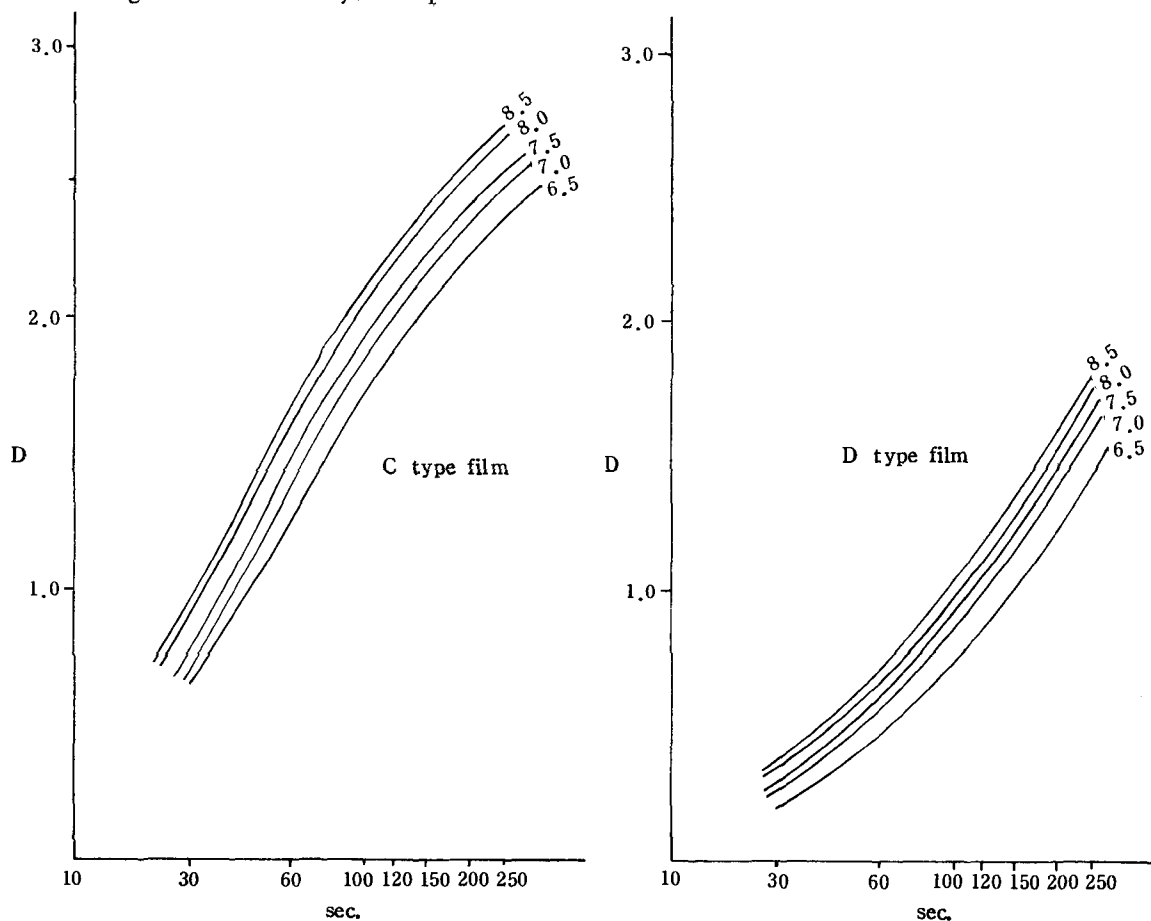


Fig. 3 Cont'd.

Table 1. The preset time established to produce  $D=1.5$  at each intensity by four kinds of films. ( Unit : seconds )

CRT intensity	Film density (D)	Single coating films												Double coating film			
		A type				B type				C type				D type			
		1.3	1.4	1.5	1.6	1.3	1.4	1.5	1.6	1.3	1.4	1.5	1.6	1.3	1.4	1.5	1.6
6.5		88	100	112	130	90	98	110	127	60	66	78	80	212	240	280	290
7.0		80	92	102	119	74	82	92	105	54	60	66	70	171	198	220	250
7.5		75	85	94	106	66	74	82	94	48	54	60	65	160	180	205	230
8.0		68	76	86	97	60	67	74	84	44	47	52	57	145	165	185	210
8.5		60	67	76	86	57	62	68	76	40	45	48	54	132	150	170	190

## 2) The proper image size settings for a given image density

Fig.4 shows the examples of images formed by adjusting the image sizes for 60 seconds at the intensity of 7.5. This imaging conditions derived from Table 1 was for a given image density of 1.5 in case of C type of film. C type of film was used in this imaging studies. As a result, the larger the image size, the lower image density. As shown in Fig.5, the image density was measured to 1.42 in the image size of 1.0, and to 1.1 in the image size of 1.2 and to 0.76 in the image size of 1.4 and to 0.66 in the image size of 1.6 and to 0.4 in the image size of 1.8 and to 0.38 in the image size of 2.0, respectively. Therefore, considering the half life of radioactivity, the proper image size settings was thought as 1.0 for the image density of  $D = 1.5$ .

## 3) The appropriate settings of the distance from the surface of the collimator for a given image density

Shown in Fig.6 are scintigrams taken at varying the distances from the face of the collimator to the phantom. All images were formed for 60 seconds at the intensity of 7.5 and the image size of 1.0 with C type film. This scintigraphic conditions selected from the experimnt 1 and 2 was for a constant image density of 1.5. As shown in Fig.7, the image density was measured to 1.42 at a distance of 0cm, to 1.29 at a distance of 5cm, to 1.30 at a distance of 10cm and to 1.29 at a distance of 15cm.

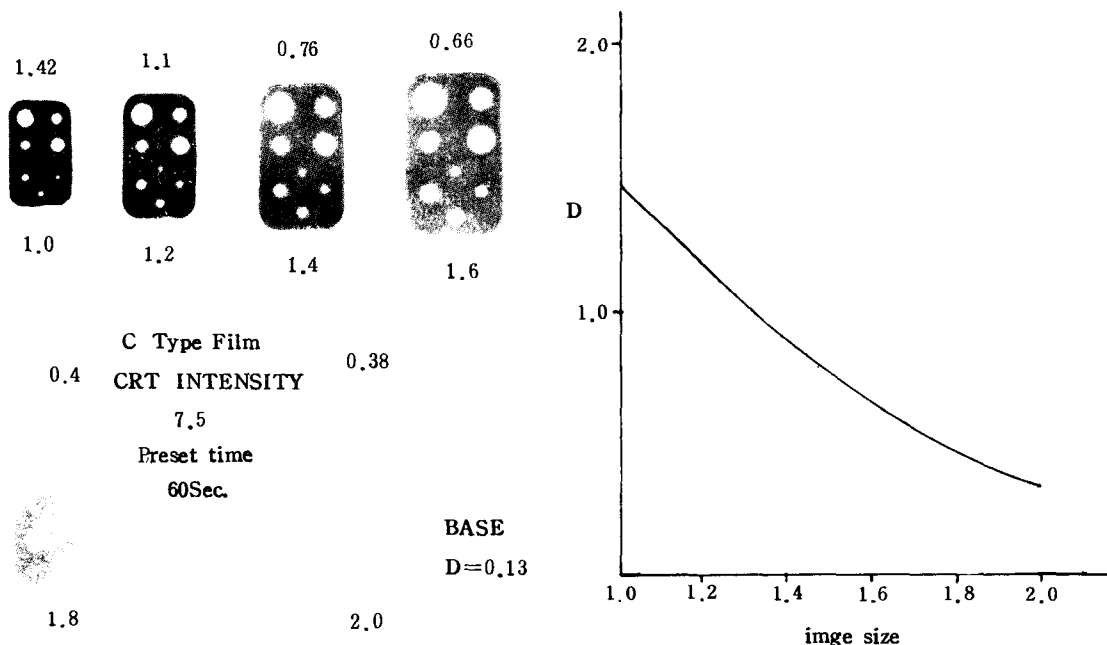


Fig. 4. Images of liver phantom obtained at different image size at the CRT intensity of 7.5

Fig. 5. Image densities versus image size for C type of film.

Although the image densities for the phantom were clearly decreased within a range of 0cm to 5cm, the image densities at a distance beyond 5cm were not approximately changed. Hence the optimum distance from the surface of the collimator to the phantom proved 0cm for the sake of unchangeable image density ( $D = 1.5$ ).

Table 2 represents the values of the density in various diameters of cold area. In general, images of cold areas were deteriorated as the phantom was moved farther away from the surface of the collimator. Thus all kinds of cold areas were generally deviated from its circular forms at a farther distance. The density levels to detect cold areas lies within a range of 0.16 to 0.73. From these results, all kinds of cold areas could be detected at a distance of 0cm, but the minimum 10mm $\phi$  cold area

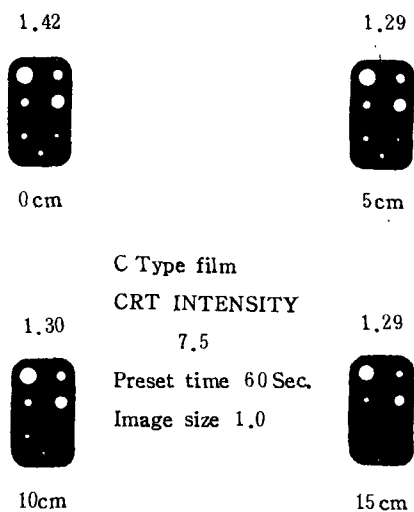


Fig. 6. Images of liver phantom taken as 0, 5, 10 and 15cm from the surface of the collimator

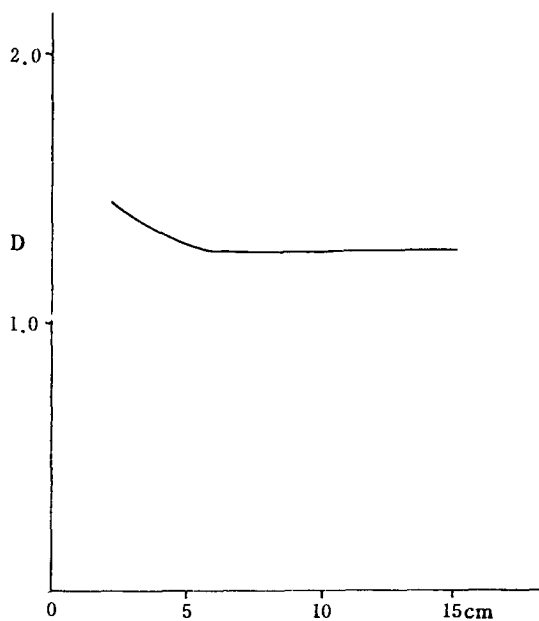


Fig. 7. Image densities as function of collimator - phantom distance for C type of film.

Table 2. Measured densities of cold areas by the distance between the surface of the collimator and the phantom

Size of cold area (mm) Distance (cm)	38	32	25	22	19	17	13	10
0cm	0.16	0.19	0.10	0.25	0.40	0.47	0.50	0.73
5cm	0.17	0.10	0.11	0.30	0.42	0.50	0.59	0.78
10cm	0.17	0.20	0.27	0.30	0.47	0.52	0.62	0.81
15cm	0.18	0.21	0.31	0.39	0.58	0.68	0.75	0.90

was indiscriminable at a distance of 5 and 10cm. Furthermore, the 10mm $\phi$  and 13mm $\phi$  cold areas at a distance of 15cm could not be identified because of backgrounds.

#### 4) The suitable window width settings for a given image density

Fig.8 demonstrates are scintiphotos taken at varying the window width. All photographings were performed for 60 seconds at the intensity of 7.5 and image size of 1.0 and the distance from the surface of the collimator of 0cm with C type film. This photographic conditions established from the experiment 1, 2 and 3 was for a given image density of  $D = 1.5$ . As illustrated in Fig.9, the image density was measured to 1.38 at the window of 15%, to 1.42 at the window of 20%, to 1.5 at the window of 30% and to 1.54 at the window of 40%, respectively. According to these facts, although the window width of 30% or 40% seems to be optimal, no image quality improvement and the detectability on cold areas could not be observed compared with 15% or 20%. Therefore, the suitable window width settings turned out 20% for a given image density of  $D = 1.5$ .

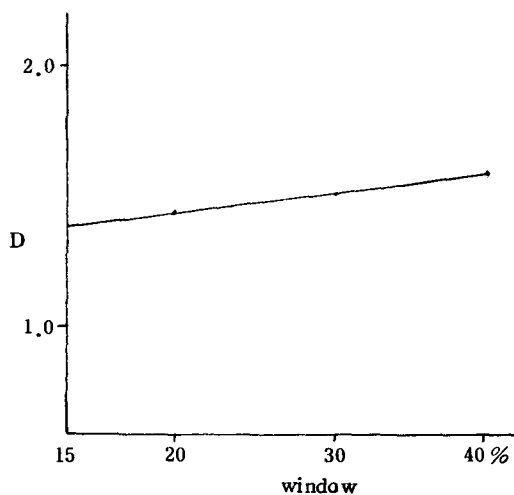
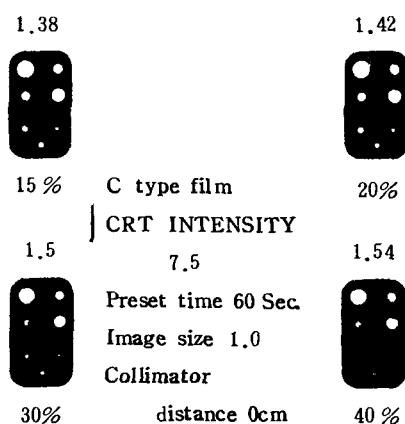


Fig. 8. Images of liver phantom obtained with four different window settings (15, 20, 30 and 40%)

Fig. 9. Image densities versus window for C type of film

Table 3. Measured densities of cold area by the window width

Size of cold area (mm) \ Window (%)	38	32	25	22	19	17	13	10
15	0.14	0.18	0.10	0.21	0.30	0.39	0.49	0.71
20	0.15	0.20	0.20	0.25	0.40	0.47	0.50	0.73
30	0.16	0.22	0.28	0.30	0.41	0.48	0.60	0.80
40	0.19	0.28	0.30	0.38	0.52	0.59	0.74	0.82



Table 3 represents the values of the density in each size of cold areas. For the most part, it is difficult to observe cold areas (10mm $\phi$ ) in the wide window width (30% and 40%). Each size of cold areas was somewhat changed from its original shape at the wider window. The density levels to detect cold areas was ranged from 0.14 to 0.74. Therefore, all kinds of cold areas could be obviously observed at the window width of 15% and 20%, but cold areas of 10mm $\phi$  could not be easily defined at the window width of 30% and 40% because of backgrounds. According to a comparison between the degrees of blurring in the cold areas by results shown in Table 2, and those of blurring in the cold areas by results shown in Table 3, it was apparent that the formers were worse than the latters.

## 5. Discussion

It is the purpose of the nuclear medicine imaging procedures to provide visual information on various processes. In all cases it is important to obtain the best images, each containing the maximum attainable informations. However, the most critical imaging studies are those involving the detection of lesion. The lesion detectability is dependent on each factor affecting imaging formation.<sup>2)</sup> It should therefore be kept in mind that by establishing an optimal imaging methodology for lesion detectability, one also maximized the performance of the system. In general, the detectability for cold lesion has a lower degree of accuracy than that of hot lesion.<sup>1,3,4)</sup> To improve the detectability for cold lesion, first of all, it should be maintained a given image density in the scintigrams. As an examples, the maximum image density within a range of 1.3 to 1.6<sup>5)</sup> or 1.5 to 1.7<sup>6)</sup> provide the best scintigrams for the liver, lung and kidney studies. Recently, due to the development of high-performance CRT, others<sup>1)</sup> have argued that image density of around 1.0 gives the good images for the detectability in cold lesions. However, since the imaging conditions for the scintigrams varies as the film types, as described in Table 1, it is necessary to evaluate the properties such as film speed, resolution, granularity and contrast, etc.<sup>7)</sup> In the case of films used in this experiment, it showed that the increase in film speed was in order of C, B, A and D type of film, the values of gamma ( $r$ ) increased in order of A, B, C and D type film. And the increase in film latitude was in order of C, A and B type film. Considering these results, a high contrast film such as A type film should be used for hot lesion detection problems, while a sensitive, low contrast film such as C type film should be used for flow studies and cold imaging.<sup>2)</sup>

Image size can also affect image information, more important, lesion detectability. When the image size is large, the image density is low. Because the larger image spreads the light dots over a larger area. So this effect should be compensated by minifying the

large size, if possible. For this reason, the 9-image and 16-image format obtained from a multiformat image system are the most frequently used for an image quality as well as lesion detectability improvement.<sup>2)</sup>

Although there are several types of collimators, but parallel multihole type collimators furnish the best combination of resolution and photopeak efficiency for many studies with a scintillation camera.<sup>8)</sup> The following are the essential characteristics of the collimator.<sup>9,10)</sup> As it were, the image size is independent of the collimator-patient distance and the spatial resolution is best at the surface of the collimator. Consequently, the face of the collimator should always be positioned as close as possible to the organ being studied, that is, touching the patient skin.<sup>9,10,11,12)</sup> Referring to the author's experimental results, the resolution of the images and the detectability of cold defects was best at the face of the collimator (0cm). But the resolution in the images was gradually degraded with an increase in collimator-phantom distance.

It should be appreciated that the proper window settings have an affect on both resolution and directly affect lesion detectability. Therefore, the technologist must select proper window width for the best image quality in the scintigrams.<sup>13)</sup> Even though a 20%<sup>14)</sup> window width for technetium 99m is normally used, 25% window width<sup>15)</sup> for it is often selected. But, by the results of this study, 15% and 20% in window width is considered to be appropriate in terms of phantom image reproduction. And the resolution of the images and the detectability for cold defects was best at the window width of 15% and especially 20%. However both of cold defects were deteriorated with an increase in window width.

## Conclusion

The results obtained from these experiments are as follows.

1. To obtain image density of  $D = 1.5$  in the case of C type of film, the proper imaging conditions was required to 60 seconds (preset time) at the intensity of 7.5, 2.0 (image size), 0cm (the face of the collimator-phantom distance) and 20% (window width).
2. The preset time of single coating films was shorter than that duplitzed film.
3. The resolution of the images was more improved in the case of the small image size, short collimator-phantom distance and narrow window width.
4. The detectability for cold defects was also improved in the case of small image size, short collimator-phantom distance and narrow window width.

## References

1. 浜田國雄, 池田穂積, 大村昌弘, 吉田梨影: シンチグラムの濃度と情報密度の検討・日放技學誌, 35(1), 67-71, 1979.
2. F. David Rollo, et. al.: Nuclear Medicine Physics, Instrumentation and Agents, 387-435, The C.V. Mosby Co., 1977.
3. 渡邊克司, 稻倉正孝: シンチレーションカメラとシンチスキャナの比較(肝腫瘍検出能を中心として)日本醫放會誌, 30, 6929, 1970.
4. 久田欣一, 油野民雄: 腹部腫瘍の核醫學診斷の進歩. 診斷と治療, 65. 1590~1600, 1971.
5. 日本アイソトープ協會: 核醫學イメージングの規格化に關する勵告. *Radioisotopes*, 28(11), 42-52, 1979.
6. RI 委員會: シンチグラム記録表示の標準化. 日放技學誌, 32(1), 44-61, 1976.
7. 藤井恭一, 前田辰夫, 前田朋行, 安河内浩: 画像診斷の體系化(頭部から上腹部まで). 180-192, ヌグプロス出版, 1981.
8. William R. Hendee: Medical Radiation Physics. 430, Year Book Medical Publishers, Inc. 1973.
9. 松本政典: Gamma Camera Image の適正撮影法(計數密度と解像力の關係及び適正 コリメータの選擇). 日放技學誌, 35(1), 72-75, 1979.
10. 慶光顯: 核醫學検査技術學. 高文社, 1981.
11. 李文錦: 臨床核醫學. 39. 麗文閣, 1982.
12. Paul J. Early, Muhammad Abdel Razzak, D. Bruce Sodee: Textbook of Nuclear Medicine Technology, 209-210, The C.V. Mosby Co. 1975.
13. F. David Rollo and Schulz, A.G.: Effects of PH selection in lesion detectability performance. *J. Nucl. Med.* 12, 690, 1971.
14. 野崎公敏: 画像診斷—考え方と進め方—, 南山堂, 1981.
15. D. Bruce Sodee, Paul J. Early: Technology and interpretation of Nuclear Medicine Procedure, 40. The C.V. Mosby Co. 1975.